



**HAL**  
open science

# A new nonlinear control for vehicle in sliding conditions: Application to automatic guidance of farm vehicles using RTK GPS

Roland Lenain, Benoit Thuilot, Christophe Cariou, Philippe Martinet

## ► To cite this version:

Roland Lenain, Benoit Thuilot, Christophe Cariou, Philippe Martinet. A new nonlinear control for vehicle in sliding conditions: Application to automatic guidance of farm vehicles using RTK GPS. IEEE International Conference on Robotics and Automation, 2004, ICRA04, Apr 2004, New Orleans, France. pp.4381-4386 Vol.5, 10.1109/ROBOT.2004.1302407 . hal-02467063

**HAL Id: hal-02467063**

**<https://inria.hal.science/hal-02467063v1>**

Submitted on 4 Feb 2020

**HAL** is a multi-disciplinary open access archive for the deposit and dissemination of scientific research documents, whether they are published or not. The documents may come from teaching and research institutions in France or abroad, or from public or private research centers.

L'archive ouverte pluridisciplinaire **HAL**, est destinée au dépôt et à la diffusion de documents scientifiques de niveau recherche, publiés ou non, émanant des établissements d'enseignement et de recherche français ou étrangers, des laboratoires publics ou privés.

# A new nonlinear control for vehicle in sliding conditions: Application to automatic guidance of farm vehicles using RTK GPS

Roland Lenain<sup>◇</sup>, Benoit Thuilot<sup>\*</sup>, Christophe Cariou<sup>◇</sup>, Philippe Martinet<sup>\*</sup>

<sup>◇</sup> Cemagref

BP50085 - 24, av. des Landais

63172 Aubière Cedex France

roland.lenain@cemagref.fr

<sup>\*</sup> LASMEA

24, av. des Landais

63177 Aubière Cedex France

benoit.thuilot@lasmea.univ-bpclermont.fr

**Abstract**—Since Global Navigation Satellite Systems are able to supply very accurate coordinates of a point (about 2 cm with a RTK GPS), such a sensor is very suitable to design vehicle guidance system. It is especially the case in agricultural tasks where a centimeter precision is often required (seeding, spraying, ...). To answer to growing high precision agriculture principle demand, several control laws for automated vehicle guidance relying on this sensor have been developed. Such guidance systems are able to supply an acceptable steering accuracy as long as vehicle does not slide (path tracking on even ground with good adherence properties...), what alas inevitably occurs in agricultural tasks. Several principles are here presented to steer vehicle whatever properties of ground and path to be followed are. In this paper a new extended kinematic model with sliding accounted is presented which allows to describe vehicle dynamics in all guidance conditions. Via this model a new non linear control law can be designed, which integrates sliding effects. Its capabilities are investigated through simulations and experimental tests.

## I. INTRODUCTION

As precision agriculture principles have been taking more and more importance in industrialized world and since improvement of GNSS (Since Global Navigation Satellite Systems) allows more and more accurate positioning data with a reducing cost, researches on automated vehicle guidance are meeting user interest, in particular in agricultural area. Moreover such systems can reduce hardness of farmer's work and improve his yield rate. As our application domain concerns vehicles working on open fields, there is no obstacle (such as buildings, or trees, ...) to disturb satellites receiving and use of a unique RTK GPS to perform a guidance task appears to be very suitable (as it has been shown in [12]).

Several research teams have been developing such systems with different performances and for dedicated applications. For the moment, only few devices are manufactured (by John Deere or CLAAS for example, ...), which are dedicated to perform specific tasks (straight line following for John Deere or harvesting for CLAAS) and can not be used for general path following. Moreover, most of them use several exteroceptive sensors (four GPS antennas in [8], RTK GPS and inertial sensor in [7], fusion between GPS and vision in [9] and [11]) to improve tracking and let control scheme be independent from sliding even if models do not take it into account.

Our approach uses only one main sensor (Real Time Kinematic GPS) which necessitates to take sliding effects into account to

preserve an acceptable tracking accuracy (as it is shown in [5]). A first idea to integrate such phenomenon inside control scheme could be the development of a dynamic model of vehicle which could take into account condition of rolling with sliding on each wheel as it has been done in [3]. Unfortunately several dynamic parameters such as tire adherence coefficient are very hard to get with sufficient accuracy and must be, in agricultural fields, evaluated on line. This can not be done efficiently in our application, and control methods have to be based on a kinematic model.

In [5], an extended kinematic model has already been designed and a new control strategy has been described and evaluated (such a control uses adaptive principles to compensate penalizing sliding effects on tracking performances). In this paper another kinematic model is described which allows to design a control, inside of which, sliding is integrated. As it is shown in this paper, this second control method with sliding accounted improves sliding compensation and presents a more control-convenient sliding point of view.

## II. EXPERIMENTAL CONTEXT

This paper deals with actual experiments carried in partnership with manufacturer CLAAS. Figure 1 shows experimental vehicles (an Ares 640 tractor from RENAULT-Agriculture and a Dominator combine harvester from CLAAS ) on which are tested control laws developed to perform automatic guidance applications. In this paper, all experiments described have been performed on tractor and control law description is relevant for the tractor (in the combine harvester case, since the steering axle is the rear one, sign modifications have to be introduced, but the control principles can be preserved). The main sensor



Fig. 1. Vehicle used for actual experiments

used to ensure control is a RTK GPS manufactured by Thales

Navigation (Aquarius 5002 unit shown on figure 2) which supplies a positioning signal, with a 2cm accuracy, at a 10Hz sampling frequency. Mobile antenna is placed on the top of the vehicle straight up the center of rear axle (since it is the vehicle control point as described in kinematic model). In addition to absolute coordinates informations, sensor system implemented on vehicle allows to access to several other data:

- Vehicle velocity: provided by GPS sensor.
- Vehicle heading: estimated via a Kalman filter which uses mobile robot evolution model fed by steering angle information and vehicle velocity.



Fig. 2. RTK GPS main sensor implemented on vehicle

### III. EXTENDED KINEMATIC MODEL

#### A. Notations

As our objective consists in path following, parameters of model are tracking oriented. Position and orientation of vehicle are so described compared to the path to be followed. Figure 3 shows this description. Vehicle is viewed as a bicycle (as in celebrated Ackermann model described for example in [13]). Parameters used to build model without sliding are hereafter listed:

- $\mathcal{C}$  is the path to be followed,
- $O$  is the center of vehicle virtual rear wheel,
- $M$  is the point on  $\mathcal{C}$  which is the closest to  $O$ .  
 $M$  is assumed to be unique, which is realistic when the vehicle remains quite close from  $\mathcal{C}$ .
- $s$  is the curvilinear coordinate of point  $M$  along  $\mathcal{C}$ , and  $c(s)$  denotes the curvature of  $\mathcal{C}$  at that point.
- $y$  and  $\tilde{\theta}$  are respectively lateral and angular deviation of the vehicle with respect to reference path  $\mathcal{C}$  (see Figure 3).
- $\delta$  is the virtual front wheel steering angle.
- $v$  is the vehicle linear velocity, considered here as a parameter, whose value may be time-varying during the vehicle evolution.
- $L$  is the vehicle wheelbase.

#### B. Sliding parameters

Notations here before described do not take into account for sliding and pseudo-sliding (due to tires deformation), which inevitably appear in our application. To build a sufficiently accurate trajectory tracking control, we have to introduce these phenomena inside model used to design control law. Figure 4 shows parameters we have chosen to describe sliding influence into kinematic model. This sliding description meets theory of vehicle dynamics partially described in [1], [2], and

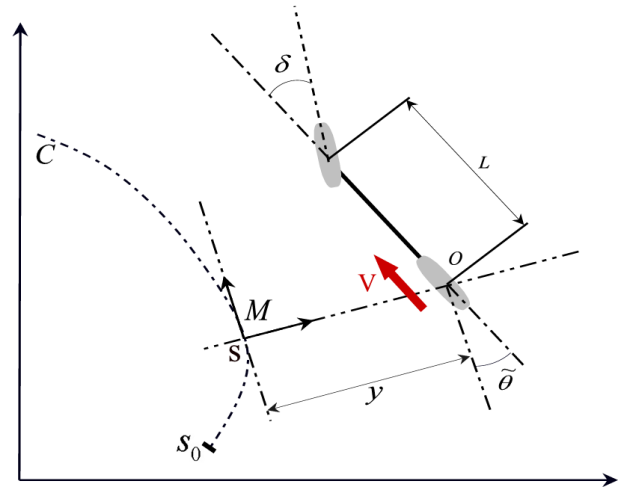


Fig. 3. Classical kinematic model parameters

behavior of a tire as described in [3].

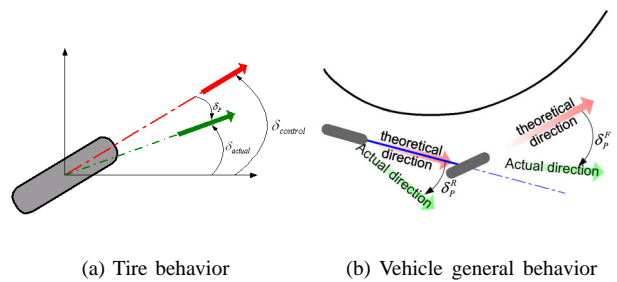


Fig. 4. Sliding parameters to be used in kinematic model

Figure 4(a) shows that the actual speed vector orientation at tire center for a given steering angle is different from direction given by this steering angle. Elasticity of tire material (pseudo-sliding) and non verification of rolling without sliding condition (skidding) generate a cornering angle called here  $\delta_P$ , which denotes difference between expected tire speed vector direction (given by steering angle) and actual one. This tire behavior modifies general vehicle dynamics as described on figure 4(b), where each of the two tires has an actual speed vector direction different from theoretical one. Instead of being a standard car like vehicle model, this description becomes closer to a two steering axles mobile robot, where front steering angle consists in an actual angle and a cornering one and rear steering angle reveals rear cornering angle.

#### C. Kinematic equations

Relying on the above remark, it can then be shown (see [6] for instance) that vehicle dynamics, described with respect to a local frame attached to the closest point of the reference path (see figure 3), can be described by equation (1).

$$\begin{cases} \dot{s} &= \frac{V \cos(\bar{\theta} + \delta_P^R)}{1 - c(s)y} \\ \dot{y} &= V \sin(\bar{\theta} + \delta_P^R) \\ \dot{\bar{\theta}} &= V \left[ \cos \delta_P^R \frac{\tan(\bar{\theta} + \delta_P^R) - \tan \delta_P^R}{L} - \frac{c(s) \cos(\bar{\theta} + \delta_P^R)}{1 - c(s)y} \right] \end{cases} \quad (1)$$

We can check that if rolling without sliding assumption is satisfied (ie  $\delta_P^F = 0$  and  $\delta_P^R = 0$ ), equation (1) fits with equation (2) which is typical kinematic model of car like vehicle without sliding (see for instance [13]).

$$\begin{cases} \dot{s} &= \frac{V \cos(\bar{\theta})}{1 - c(s)y} \\ \dot{y} &= V \sin(\bar{\theta}) \\ \dot{\bar{\theta}} &= V \left[ \frac{\tan(\bar{\theta})}{L} - \frac{c(s) \cos(\bar{\theta})}{1 - c(s)y} \right] \end{cases} \quad (2)$$

Models (1) and (2) exist under condition  $y \neq \frac{1}{c(s)}$ , which occurs when point  $O$  on figure 3 (control point) is superposed with reference path center of curvature. This is never the case in experiments, since the vehicle remains close to reference path.

#### D. Sliding parameters estimation

One main problem in the approach chosen is estimation of sliding. The two parameters here before introduced have to be estimated online, as they are not constant, due to various and time varying parameters (steering angle, ground properties, slope, ...). Moreover, since we use a unique exteroceptive sensor, we assume that all vehicle dynamics can be described with model (1). Several dynamic behavior are so ignored in model (such as roll or pitch) but their effects on path tracking accuracy are considered negligible in front of sliding.

As we can access to all other parameters via direct measurement or reconstruction, we are able to evaluate  $\delta_P^R$  and  $\delta_P^F$  through calculations on model (1). Computation gives us the result presented in equation (3).

$$\begin{cases} \delta_P^R &= \arcsin\left\{\frac{y^k - y^{k-1}}{V \cdot T_e}\right\} - \tilde{\theta}^k \\ \delta_P^F &= \arctan\left\{\frac{L}{V \cos \delta_P^R} \frac{\theta^k - \theta^{k-1}}{T_e} + \tan \delta_P^R\right\} - \delta^k \end{cases} \quad (3)$$

where,  $\theta$  is the absolute vehicle heading while  $\tilde{\theta}$  is heading deviation with respect to reference path.  $X^k$  denotes a variable obtained by measure at time  $k * T_e$  where  $T_e$  is the sample time (here 0.1s). In equation (3), arcsin exists under the condition:

$$|y^k| < V \cdot T_e + |y^{k-1}| \quad (4)$$

which is equivalent, in the continuous case to  $|\dot{y}| < V$ . Condition (4) denotes that lateral velocity (with respect to reference path) is lower or equal than vehicle velocity. This is not physically possible, as described by model (1). As models are expected to be fed by actual signals, condition (4) can be viewed as a tool which can reduce misestimation of sliding parameters (in particular due to movements of antenna linked to the motion of tractor cabin with respect to rear axle).

#### E. Steering law design without sliding accounted

It has been established that most of mobile robots kinematic models can be converted, *without any approximation*, into almost linear models named chained forms, see for instance [10]. Such an approach is attractive, since control laws can then be designed according to Linear Systems Theory, while still relying upon the actual nonlinear mobile robots kinematic models.

More precisely, nonlinear kinematic model is first converted into chained form via invertible state and control nonlinear transformations. A linear control law is then designed relying on the chained form. Finally, the actual control law is computed via state and control nonlinear transformations. In [12], this technique is applied to kinematic model (2). It is shown that curved path following (i.e. maintaining  $y$  and  $\bar{\theta}$  equal to 0) can be achieved according to nonlinear control law:

$$\delta(y, \tilde{\theta}) = \arctan \left( L \left[ \frac{\cos^3 \tilde{\theta}}{(1 - c(s)y)^2} \left( \frac{d c(s)}{d s} y \tan \tilde{\theta} - K_d (1 - c(s)y) \tan \tilde{\theta} - K_p y + c(s)(1 - c(s)y) \tan^2 \tilde{\theta} \right) + \frac{c(s) \cos \tilde{\theta}}{1 - c(s)y} \right] \right) \quad (5)$$

Where  $K_p$  and  $K_d$  can be interpreted as parameters of a PD controller. The new control law proposed in this paper will be exposed in section V.

## IV. MODEL VALIDATION

#### A. Previous sliding model

1) *Description*: To compare results supplied by this sliding accounted method, here is briefly presented a previous model detailed in [5]. This model was obtained by adding two sliding parameters,  $\dot{Y}_p$  and  $\dot{\Theta}_p$ , inherited from dynamic vehicle analysis to model (2) (without sliding):

$$\begin{cases} \dot{s} &= \frac{v \cos \bar{\theta}}{1 - c(s)y} \\ \dot{y} &= v \sin \bar{\theta} + \dot{Y}_p \\ \dot{\bar{\theta}} &= v \left( \frac{\tan \delta}{L} - \frac{c(s) \cos \bar{\theta}}{1 - c(s)y} \right) + \dot{\Theta}_p \end{cases} \quad (6)$$

Evaluation on line of these parameters is made in a similar way than one leading to equation (3).

2) *Comparison between models*: The new sliding model (1) denotes that sliding occurring during agricultural tasks is due to own vehicle movement and is linked to vehicle velocity. On the contrary, in previous model (6), sliding parameters are independent from vehicle configuration, so there is no mathematical restriction (such as condition (4)) on sliding parameters in that model: it allows therefore the vehicle to be submitted to sliding effects which can not be compensated (i.e.  $|\dot{Y}_p| > |v \sin \bar{\theta}|$ , phenomenon which is not addressed in our applications).

When condition (4) is satisfied, it is possible to obtain mathematical relations (depending on vehicle configuration  $\bar{\theta}$  and  $\delta$ ) between the two sets of sliding parameters: this shows equivalence of models (1) and (6) (corroborated by simulation with theoretical sliding parameters).

The main difference between the two models is the integration level of sliding effects inside vehicle description: it acts

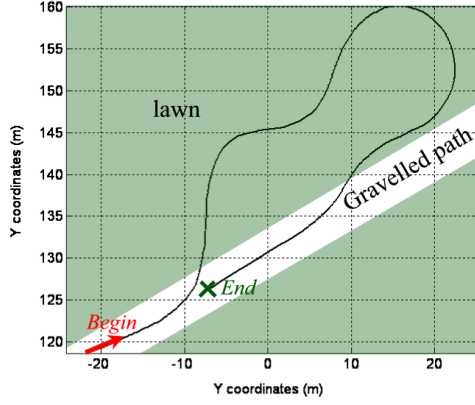


Fig. 5. Actual Path followed to validate models

on how sliding is viewed and can be corrected. While sliding effects in model (6) are accounted by adding parameters on vehicle motion equations, they are integrated in nonlinear evolution equations in model (1). From a control point of view, the advantage of this second model is that it is in a suitable form to be exactly linearized (chained system) with sliding accounted.

### B. Validation and comparison relying on actual experiments

As a mathematical relation exists between sliding parameters of the two models, simulations with theoretical conditions provide exactly the same results. Here are now described results of sliding models simulation fed on-line during an actual path following, achieved with control law without sliding accounted (5). Actual measurement data feed equation (3) to evaluate sliding parameters, which are injected in an on-line simulator to provide a simulated lateral deviation using both of sliding models. Figure (5) depicts path followed. Results are presented on figure 6 where are depicted :

- in green dashed dot line, the vehicle actual lateral deviation during the path following,
- in blue solid line, simulation relying on previous model (6)
- in black dashed line, simulation relying on new model (1)

We can see that the three lateral deviations depicted are very close. The two sliding models are so able to describe with accuracy vehicle dynamics, what is a first step to take it into account in control design. the slight differences between simulation of the two models are due to sliding estimation algorithms which do not compute sensor noise in the same way.

## V. CONTROL DESIGN

Previous model (6) has been used to develop an adaptive control law relying on a moving reference : the control law is (5) designed under non sliding assumptions. However, instead of specifying a null expected lateral deviation, lateral deviation with sliding, online simulated or calculated, is specified as new expected deviation (see scheme depicted on

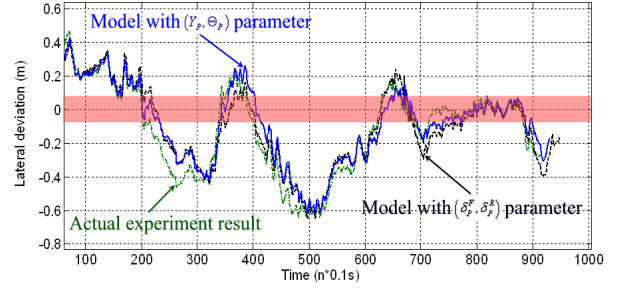


Fig. 6. Comparison between models and actual vehicle dynamics

figure 7). Convergence of lateral deviation to 0 in presence of sliding is ensured if sliding is constant. Lateral deviation with respect to the path to be followed is considerably reduced when sliding is not constant (this adaptive principle is detailed and experimentally tested in [5]).

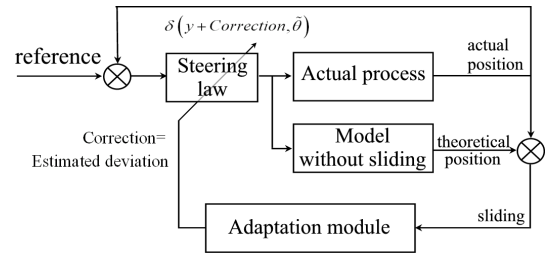


Fig. 7. Scheme of previous control method

An alternative control design is now proposed. It is shown hereafter that new sliding modeling (ie model (1)) provides equations which can be turned into a "chained system". Sliding effects can then be introduced inside a nonlinear control law to provide system with faster reaction and an improved robustness.

### A. Chained system conversion

As developed in [10], one way to build a nonlinear suitable control law for mobile robots is to turn their equations into chained form (as it has been done, in order to design control law (5)). In dimension 3 (as expected in our application), such a system is given by :

$$\begin{cases} \dot{a}_1 = m_1 \\ \dot{a}_2 = a_3 m_1 \\ \dot{a}_3 = m_2 \end{cases} \quad (7)$$

where  $A = [a_1, a_2, a_3]^T$  and  $M = [m_1, m_2]^T$  are resp. the state and control vectors. One can check that such a system is almost linear: just replace time derivation by a derivation with respect to  $a_1$ . It leads to system (8) (with notation  $a'_i = \frac{da_i}{da_1}$ ).

$$\begin{cases} a'_1 = 1 \\ a'_2 = a_3 \\ a'_3 = m_3 = \frac{m_2}{m_1} \end{cases} \quad (8)$$

By analogy with chained transformations proposed for car like vehicle in the rolling without sliding case (see for instance [10]), the following state transformation  $(s, y, \theta) \rightarrow$

$(s, y, \tan(\tilde{\theta} + \delta_P^R)) [1 - c(s)y]$  is here proposed in association with control transformation given by (9):

$$\begin{cases} m_1 = \frac{V \cos(\tilde{\theta} + \delta_P^R)}{1 - c(s)y} \\ m_2 = \frac{d}{ds} \left( \tan(\tilde{\theta} + \delta_P^R) [1 - c(s)y] \right) \end{cases} \quad (9)$$

According to equation (9), calculation of control  $m_2$  implies derivation of sliding parameter  $\delta_P^R$ . However,  $\delta_P^R$  is estimated via equation (3), which already requires calculations similar to derivation. This parameter appears therefore to be very noisy, and another numerical derivation (as we have no analytical expression) would not be convenient in a steering law. Moreover, during most of the guidance operations (straight line following, constant curvature following or on slope) sliding is almost constant or slowly varying. Important variations in sliding parameters occur only at the beginning or the ending of a curve, where sliding is not a preponderant phenomenon. Therefore, we assume here that parameter  $\delta_P^R$  is constant (ie  $\dot{\delta}_P^R = 0$ ). Using this hypothesis, calculation of  $m_2$  gives us:

$$\begin{aligned} m_2 = & -c(s)V \sin(\tilde{\theta} + \delta_P^R) \tan(\tilde{\theta} + \delta_P^R) \\ & + \frac{1-c(s)y}{\cos^2(\tilde{\theta} + \delta_P^R)} V \left[ \cos \delta_P^R \left( \frac{\tan(\delta + \delta_P^R) - \tan \delta_P^R}{L} \right) \right. \\ & \left. - \frac{c(s) \cos(\tilde{\theta} + \delta_P^R)}{1-c(s)y} \right] \end{aligned} \quad (10)$$

Equation (10) exists under the same conditions than those obtained in the rolling without sliding case:  $V \neq 0$ ,  $y \neq \frac{1}{c(s)}$  and  $\tilde{\theta} \neq \frac{\pi}{2} [\pi]$ . These conditions are assumed to be satisfied in practical experiments.

### B. Control law design

Since kinematical model (1) with sliding accounted is validated and can be turned into chained form (8), a natural expression for the virtual control law is:

$$m_3 = -K_d a_3 - K_p a_2 \quad (K_p, K_d) \in \mathbb{R}^{+2} \quad (11)$$

since it insures that  $a_2$  obeys the following equation:

$$a_2'' + K_d a_2' + K_p a_2 = 0 \quad (12)$$

Equation (12) establishes the following convergences :

- $a_2 \rightarrow 0$ : this is equivalent to  $y \rightarrow 0$  (according to the state transformation) and ensures convergence of the vehicle to the path to be followed (null lateral deviation).
- $a_3 \rightarrow 0$ : this implies (according to the state transformation) that  $\tilde{\theta} \rightarrow \delta_P^R$ . This condition shows that the vehicle heading will not be parallel to the reference path tangent, but will compensate effect of rear cornering angle to ensure the convergence of lateral deviation to zero.

The actual control variable is vehicle steering angle. It can be obtained by reporting (10) in (11), and inverting the resulting relation. We obtain :

$$\delta = \arctan \left\{ \frac{L}{\cos \delta_P^R} \left[ c(s) \frac{\cos \tilde{\theta}_2}{\alpha} + A \frac{\cos^3 \tilde{\theta}_2}{\alpha^2} \right] + \tan \delta_P^R \right\} - \delta_P^R \quad (13)$$

$$\text{where: } \begin{cases} \tilde{\theta}_2 = \tilde{\theta} + \delta_P^R \\ \alpha = 1 - c(s)y \\ A = -K_d \alpha \tan \tilde{\theta}_2 - K_p y + c(s) \alpha \tan^2 \tilde{\theta}_2 \end{cases} \quad (14)$$

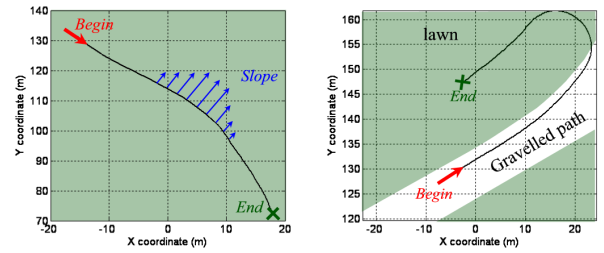
We can notice that the two sliding parameters appear in the expression of nonlinear control law (13). Both of the cornering angles (which describe sliding effects) are taken into account and can also be compensated.

Performances of such a control law can be adjusted by tuning gains  $K_p$  and  $K_d$  which can be viewed as proportional and derivative actions of a linear controller. Since there is no restriction on arctan function, control  $\delta$  can vary inside  $]-\frac{\pi}{2}, \frac{\pi}{2}[$ . Consequently, saturations and performances of actuators are to be considered when tuning gains. In experimental results hereafter detailed, gains are set to values (15). They impose a convergence to the reference path within 15m, without overshoot.

$$\begin{cases} K_p = 0.09 \\ K_d = 0.6 \end{cases} \quad (15)$$

## VI. EXPERIMENTAL RESULTS

### A. Reference path



(a) Straight line on slope

(b) Half circle

Fig. 8. Actual paths to be followed

The first experimental results with control law (13) are here below described. They consist in straight line following on a sloping field at  $4km.H^{-1}$  (figure 8(a)) and in curve following on an even sloppy ground at  $7km.H^{-1}$  (figure 8(b)). Ground on which vehicle has run is gravel or lawn as depicted on figure 8. These two paths are representative of guidance conditions during sliding appears and reduces trajectory tracking accuracy. Performances are compared with control law without sliding accounted (5) and adaptive control scheme described in [5].

### B. Results

Figure 9 depicts the straight line following on sloping ground. Classical control without sliding accounted makes vehicle converge up to a non null deviation during slope (ie when sliding occurs). On the contrary, with previous and new control laws, lateral deviation comes back to zero during slope. Their performances are very similar: as slope appears, one can observe a transient deviation before sliding models can supply relevant information.

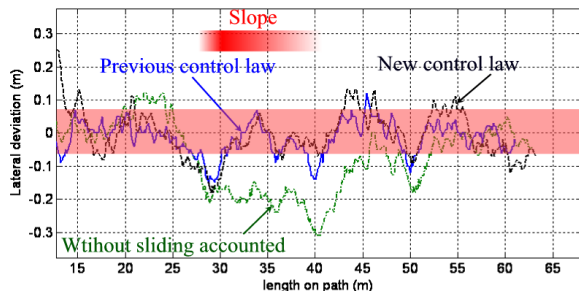


Fig. 9. Lateral deviation during sloping path following

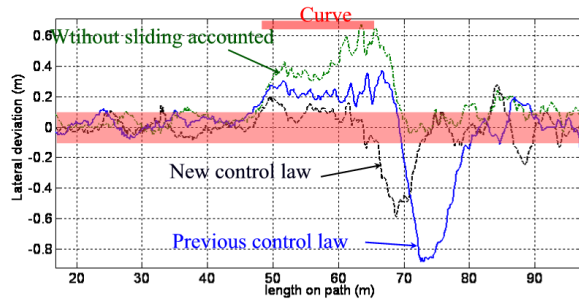


Fig. 10. Lateral deviation during curved path following

Such a delay to calculate relevant values for sliding parameters when these latter change quickly appears more significantly on figure 10 at the beginning and the ending of the curve. At such times, curvature introduces a step on sliding parameters, and the brief non negligible lateral deviation observed is due to control laws settling time. This effect is amplified as rear sliding parameter  $\delta_P^R$  is assumed to be constant as described in  $m_2$  calculation (see equation (10)). Sliding effects are then significantly compensated during the curve, but overshoots at transient phases have now to be addressed.

It can however be noticed that new control law (13) is able to react faster since sliding parameters are included inside nonlinear control calculation. In this critical path following where curvature radius is close to tractor maximal one (steering angle control  $\delta$  goes up to  $40^\circ$ ), the less reactive method (previous control) is not able to steer the tractor to a null lateral deviation during such a curve.

## VII. CONCLUSION AND FUTURE WORKS

In this paper a new vehicle kinematic model accounting for sliding effects is described. It has been shown that it can fit with actual vehicle dynamics and is equivalent to model described in [5]. However the model structure allows to design a control scheme which integrates sliding inside nonlinear control law. This new method improves accuracy of guidance system, robustness and reactivity.

One limitation of such a law is the impact of noise resulting from vehicle dynamical movement (cabin oscillation, since GPS antenna is located on the top of the tractor). Butterworth

filters are presently used to smooth sliding parameters estimation, but they are not fully satisfactory. Another critical point appears when sliding parameters are quickly modified (typically at the beginning/ending of a curve). Since rear sliding parameters  $\delta_P^R$  is assumed to be constant in model conversion (see equation (9)), and considering time delay due to sliding estimation and low level actuator capacities, a transient deviation then occurs.

Current developments are focused on these problems. Predictive control methods are investigated to take into account time varying sliding and low level delay to eliminate overshoot problems especially in curve. Adaptive filters are in development to reject parasite dynamical movements which depend on ground conditions and configuration of tractor (implement loaded on tractor...). Such additional principles will have to improve guidance control in presence of sliding in all tractor configurations and for any paths to be followed, ground conditions, to meet farmer expectations (about  $\pm 5cm$ ).

## REFERENCES

- [1] Ackermann J. *Robust Lateral and Yaw Control*. In Proc. of Eur. summer school in automatic control, Grenoble (France), 2002.
- [2] Dormegnie E., Fandard G., Mahajoub G., Zarka F. *Dynamique du véhicule*. Lectures at French Institute for Advanced Mechanics (IFMA), 2002.
- [3] Ellouze M. and d'Andréa-Novel B. *Control of unicycle-type robots in the presence of sliding effects with only absolute longitudinal and yaw velocities measurement*. In European Journal of Control, 6:567-584, 2000.
- [4] Holzhüter T. and Schultze R. *Operating experience with a high-precision track controller for commercial ships*. In Control Engineering Practice 4(3):343-350, 1996.
- [5] Lenain R., Thuilot B., Cariou C. and Martinet P. *Adaptive control for car like vehicles guidance relying on RTK GPS: rejection of sliding effects in agricultural applications*. In Proc. of the Intern. Conf. on Robotics and Automation (ICRA), Taipei, Sept. 2003.
- [6] Micaelli A., Samson C. *Trajectory tracking for unicycle-type and two-steering-wheels mobile robots*. INRIA research report Number 2097, Nov. 1993.
- [7] Nagasaka Y., Otani R., Shigeta K. and Taniwaki K. *Automated operation in paddy fields with a fiber optic gyro sensor and GPS*. In Proc. of the Intern. Workshop on Robotics and Automated Machinery for Bio-Productions (Bio-Robotics), pp 21-26, Valencia (Spain) September 1997.
- [8] O'Connor M., Elkaim G., Bell T. and Parkinson B. *Automatic steering of a farm vehicle using GPS*. In Proc. of the 3<sup>rd</sup> Intern. Conf. on Precision Agriculture, Minneapolis (USA), pp 767-777, June 1996.
- [9] Ried J. and Niebuhr D. *Driverless tractors*. In Ressource 8(9):7-8, September 2001.
- [10] Samson C. *Control of chained systems. Application to path following and time-varying point-stabilization of mobile robots*. In IEEE Trans. on Automatic Control 40(1):64-77, January 1995.
- [11] Stentz A, Dima C, Wellington C, Herman H, Stager D *A system for semi-autonomous tractor operations* in Autonomous robots 13(1):87-104, 2002.
- [12] Thuilot B., Cariou C., Martinet P. and Berducat M.. *Automatic guidance of a farm tractor relying on a single CP-DGPS*. In Autonomous robots 13(1):53-71, July 2002.
- [13] The Zodiac. *Theory of robot control*. Canudas de Wit C., Siciliano B. and Bastin G. eds, Springer Verlag, Berlin (Germany) 1996.